Computers, Materials & Continua CMC, vol.65, no.3, pp.2385-2396, 2020

A Novel Edge Computing Based Area Navigation Scheme

Jianzhong Qi[1, 2, *], Qingping Song[3] and Jim Feng[4]

Abstract: The area navigation system, discussed in this paper, is composed of ground responders and a navigation terminal and can position a high-velocity aircraft and measure its velocity. This navigation system is silent at ordinary times. It sends out a request signal when positioning is required for an aircraft, and then the ground responders send a signal for resolving the aircraft. Combining the direct sequence spread spectrum and frequency hopping, the concealed communication mode is used in the whole communication process, with short communication pulses as much as possible, so the system has strong concealment and anti-interference characteristics. As the transmission delay is apparent in the response communication mode, there is a big error where the common navigation algorithm is used for the positioning and velocity measurement of a high-velocity aircraft. In this paper, a new algorithm is proposed, which can eliminate the influence of response communication delay on the positioning of a high-velocity moving target to realize the precise positioning and velocity measurement of a high-velocity aircraft.

Keywords: Navigation, pseudo-noise code ranging, positioning, velocity measurement, edge computing.

1 Introduction

Navigation refers to the process of acquiring the information about the position, velocity, and time of carriers. Common navigation systems include an inertial navigation system, satellite navigation system, astronomical navigation system, and other navigation systems using a magnetic field, optics, and radio. With great progress, the satellite navigation system has been successfully applied in many fields such as military and civilian use since the 1990s [Elliott and Hegarty (2006)]. Various aircraft are increasingly dependent on the satellite navigation system, but the satellite navigation system is extremely susceptible to interference due to its openness. The interference and deception against the

[1] School of Information Science and Technology, North China University of Technology, Beijing, 100144, China.

[2] School of Computer and Communication Engineering, University of Science and Technology Beijing, Beijing, 100083, China.

[3] Science and Technology on Information Systems Engineering Laboratory, Beijing Institute of Control and Electronic Technology, Beijing, 100038, China.

[4] Amphenol Global Interconnect Systems, San Jose, CA 95131, USA.

[*] Corresponding Author: Jianzhong Qi. Email: qijianzhong2002@aliyun.com.

Received: 22 May 2020; Accepted: 10 July 2020.

satellite navigation system are an important part of electronic warfare.

So a better solution is required to solve these problems. In recent years, some computing patterns based on network edge have been proposed to address the distributed computing tasks, such as edge computing [Lin, Zhou, An et al. (2018); Gong, Lin, Gong et al. (2020), Hui, Zhou, Xu et al. (2020); Wang, Kong, Li et al. (2019); Medhane, Sangaiah, Hossain et al. (2020); Tang, Wang, Song et al. (2019)] and fog computing [Lin, Zhou, Pau et al. (2018); An, Lü, Yang et al. (2019)]. To overcome the shortcomings of the satellite navigation system, the ground-based area navigation and positioning system (GANP) based on edge computing is proposed in this paper. As shown in Fig. 1, it mainly includes two parts, namely the ground responder part and aircraft. The GANP works in the edge computing mode. Firstly, the aircraft sends a positioning request to the edge responders. Secondly, the edge responders send their position coordinates to the aircraft respectively. Lastly, the aircraft computes its position using these data.

The area navigation system, working independently of the satellite navigation system, has been researched more and more in different countries. A pseudolite-based concealed navigation system used in electronic warfare environments is studied in this paper, which can position a high-velocity aircraft. Such a navigation system is silent at ordinary times. It sends out a request signal when positioning is required, and then the ground station transmits a signal for positioning the aircraft. Combining the spread spectrum and frequency hopping, the concealed communication mode is used in the whole communication process, with short communication pulses as much as possible, so that the communication signal is undetectable.

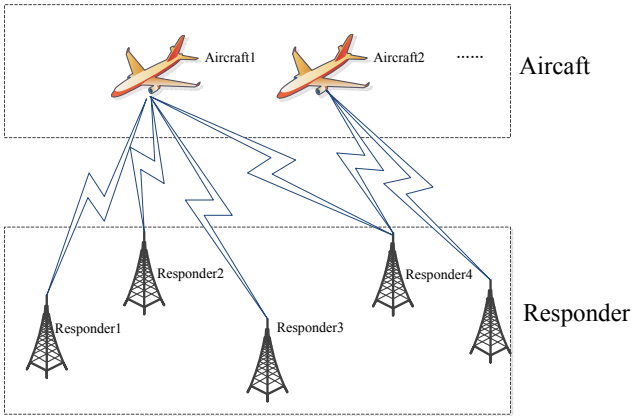

Figure 1: Block diagram for the composition of a response-type ground-based navigation system

This paper, from the perspective of engineering application, discusses the working principle and positioning accuracy of the concealed ground-based area navigation system and has a certain guiding significance for practical application of such a navigation system.

The structure of this paper is as follows. In Section 2, the ranging method of this system is discussed. In Section 3, the methods of estimating the PN-code phase and carrier frequency required in the ranging process are introduced. In Section 4, the method of

computing the position of the system after the ranging is completed is introduced. In Section 5, the method of calculating the velocity of the system is described. In Section 6, the frequency-hopping communication method of the system is introduced. The paper is concluded in Section 7.

2 Response-type pseudo-noise code ranging method

2.1 Response-type incoherent pseudo-noise code ranging steps

The navigation system studied herein is composed of an aircraft navigation terminal and ground responders. In principle, ground stations are arranged in the accurately measured sites on the earth's surface, and the position and velocity of an aircraft can be calculated by measuring the distance between the aircraft and each ground station using the navigation terminal. Different ground responders of this system work in the manner of code division multiple access (CDMA), that is, different PN-codes are used for different ground responders, and the PN-codes of uplink signals are different from those of downlink ones; the response-type PN-code ranging mode is adopted to measure the distance between the ground responders and the aircraft.

The response-type PN-code ranging process herein is as follows:

Step 1: The aircraft navigation terminal transmits a downlink spread spectrum pseudo-random signal at t_1 (downlink signal frame header time);

Step 2: Upon receiving of the downlink signal, the ground responders start to transmit an uplink spread spectrum signal at t_0, and the navigation message of the uplink signal includes the transponding circuit delay τ of responders, uplink transmission moment t_0, PN-code phase Φ_1 from the downlink frame header at t_0, etc.;

Step 3: The aircraft navigation terminal receives the uplink signal from different responders, captures the PN-codes, estimates the PN-code phase, and demodulates the navigation message;

Step 4: The PN-code phase Φ_2 from the uplink frame header at t_2 is estimated at the next sampling moment t_2 of the aircraft navigation terminal;

Step 5: The distance is obtained through calculating the transmission time of radio wave in the air according to the time when the uplink signal frame header arrives at the missile-borne processor, the transponding circuit delay τ of responders, and the PN-code phase Φ_1 from the downlink frame header at the uplink transmission moment.

The principle of response-type incoherent PN-code ranging is analyzed as below. If the clock bias between the aircraft navigation terminal and the ground responder is Δt, the channel delay is τ and the PN-code rate is Rc, then the transmission moment of the aircraft navigation terminal for the signal received by the ground responder at t_0 is t_1-Φ_1. The moment when the signal received by the aircraft navigation terminal at t_2 leaves the ground responder is t_0-Φ_2. The following equations can be presented:

$$\begin{aligned} L_1 &= \left(t_0 - (t_1 - \phi_1) - \Delta t - \tau\right) \times c \\ L_2 &= \left(t_2 - (t_0 - \phi_2) + \Delta t - \tau\right) \times c \end{aligned} \tag{1}$$

The following is obtained from the equations above:

$$L_1 + L_2 = (t_2 - t_1 + \phi_1 + \phi_2 - \tau_\Sigma) \times c \tag{2}$$

If the distance between the aircraft and the ground responder at t_1 is L_1, that between the aircraft and the ground responder at t_2 is L_2, and that between the aircraft at t_2 and the aircraft at t_1 is L_3, then the relationship among their positions is as shown in the Fig. 2 below:

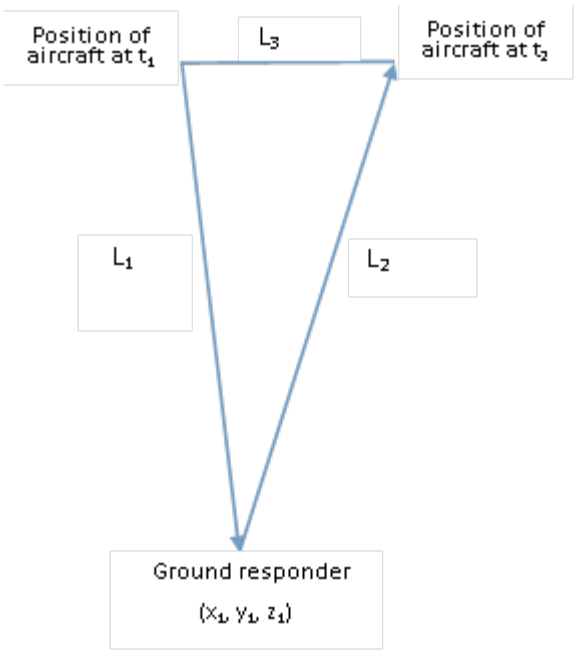

Figure 2: Relative positions between aircraft and ground responder

The short-pulse response communication mode is used. Owing to the shorter time, the flight velocity of the aircraft does not change during the response communication, and the radial velocity *Vr* between the aircraft navigation terminal and ground station can be calculated by the Doppler frequency. The following equations can be presented:

$$L_1 - L_2 = (t_2 - t_1 + \phi_1 + \phi_2 - \tau_\Sigma) \times V_r \tag{3}$$

The following is obtained, therefore:

$$L_1 = \frac{1}{2}(c + V_r)(t_2 - t_1 + \phi_1 + \phi_2 - \tau_\Sigma) \tag{4}$$

2.2 Estimation of the radial velocity between the aircraft navigation terminal and ground responder

As shown in Eq. (4) above, it is necessary to calculate the radial velocity *Vr* between the aircraft and ground station in order to obtain the distance L_1 between the aircraft and ground station. This system realizes the estimation of the Doppler frequency of communication carrier wave by the aircraft navigation terminal using the method of carrier wave coherent transponding, and accordingly, the radial velocity between the aircraft and ground station can be estimated. If the carrier frequency of the downlink signal of the aircraft navigation

terminal is f_{DOWN}, the carrier Doppler shift of the downlink signal is $f_{dopplor}$, the carrier frequency of the uplink signal of the responder is f_{up}, and the ratio of the uplink carrier frequency to the downlink carrier frequency of the responder is set as S, then the functional block diagram of the responder is as shown in Fig. 3 below:

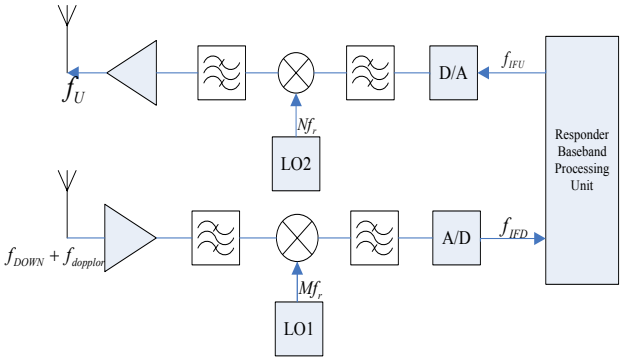

Figure 3: Block diagram for the frequency conversion of ground responder

The carrier frequency of the downlink signal received by the ground responder shall be $f_{DOWN}+f_{dopplor}$. If the responder-received radio frequency is converted into intermediate frequency under the channel as f_{IFD}, then

$$f_{IFD} = f_{DOWN} + f_{dopplor} - Mf_r \tag{5}$$

The value of the intermediate frequency f_{IFD} is estimated accurately in the baseband processing unit of the responder, and the intermediate frequency f_{IFU} of the uplink carrier is S times of f_{IFD}, namely coherent transponding.

$$f_{IFU} = Sf_{IFD} = S(f_{DOWN} + f_{dopplor} - Mf_r) \tag{6}$$

Selecting the appropriate local oscillation frequency of receiving and transmission frequency channels, there is $-SMf_r + Nf_r = 0$, namely $S = \frac{N}{M}$. The carrier frequency of the uplink signal transmitted by the ground responder shall be f_U, as shown in the equation below:

$$f_U = S(f_{DOWN} + f_{dopplor}) \tag{7}$$

It can be seen from the equation above that the responder selects the appropriate local oscillation frequency and performs coherent transponding for the intermediate frequency and the uplink frequency of the responder will be S times of the receiving frequency and unrelated to the local reference oscillator. This is an important advantage of the system: the reference frequency of the entire system is locked on the missile-borne reference frequency source, and it is unrelated to the frequency source of each ground responder, thus improving the frequency stability of the system and reducing the computational complexity.

According to the formula of Doppler frequency

$$f_{doppler} = \frac{v}{c} f_{DOWN} \tag{8}$$

The short-pulse response communication mode is used. Owing to the shorter time, the

flight velocity of the aircraft does not change during the response communication, and the carrier frequency of the uplink signal received by the aircraft navigation terminal from the ground responder is as follows:

$$\begin{aligned} f_R &= f_U + \frac{v_r}{c} f_U \\ &= S(f_{DOWN} + f_{dopplor}) + \frac{v_r}{c} S(f_{DOWN} + f_{dopplor}) \end{aligned} \tag{9}$$

As the flight velocity on the ground is far lower than the velocity of light, $\frac{v_r}{c} Sf_{dopplor}$ is negligible, and then

$$f_R \approx Sf_{DOWN} + 2Sf_{dopplor} \tag{10}$$

The Doppler shift of the downlink carrier can be calculated.

$$f_{doppler} \approx \frac{f_R - Sf_{DOWN}}{2S} \tag{11}$$

According to Eqs. (8) and (11), the radial velocity *Vr* between the aircraft and ground responder can be calculated as follows:

$$V_r = \frac{f_{doppler}}{f_{DOWN}} c = \frac{f_R - Sf_{DOWN}}{2S} \frac{c}{f_{DOWN}} \tag{12}$$

According to Eq. (12), the radial velocity between the aircraft and ground station can be calculated if the aircraft navigation terminal accurately estimates the frequency of the received uplink signal.

3 Estimation of PN-code phase and carrier frequency

As mentioned above, the ground responder and aircraft navigation terminal shall accurately estimate the carrier frequency and PN-code phase of the downlink signal and uplink signal, respectively, in order to perform ranging calculations. The PN-code phase and carrier frequency can be estimated through rough estimation and fine estimation in succession. The rough estimation for the signal PN-code phase and the carrier frequency of the DSSS-modulated signal means that the estimated accuracy of the PN-code phase is less than that of half PN-code chip. The accuracy of carrier Doppler is 2/Tc, and this process is usually called as signal capturing in the spread spectrum communication.

3.1 Rough estimation of the PN-code phase and carrier frequency

Common algorithms of PN-code and carrier capture include a sliding correlation method, FFT-IFFT method, and partial matched filter (PMF)+FFT algorithm. Among them, the PMF+FFT capture algorithm can achieve the capture of the PN-code phase and carrier frequency in one PN-code period, without searching the carrier sweep frequency. Therefore, the PMF+FFT capture algorithm is the fastest among the three capture algorithms discussed above, and thus it is selected for this topic [Qi, Luo and Song (2014)].

The partial matched filter (PMF) method divides a complete sequence of a longer period

into several smaller sequences to obtain the results of each partially matched filter by segmented matching. The principal structure of the PMF+FFT capture method is as shown in Fig. 4. The part in the dotted circle is a partially matched filter (PMF), each PMF outputs a partially coherent cumulative sum to the N point FFT operation module at each moment of sliding, the FFT is used to perform spectrum analysis on the partial results of matched filtering at each moment, and the capture results are judged based on the frequency spectrum. As long as the input signal contains the same spread spectrum code sequence as the local one, there is always a moment when the two signals are aligned in the code phase during matching, however, the correlation peak value may not be detected due to the carrier deviation. When the input sequence is aligned with the local sequence, the PN-codes have been offset, and only the carrier deviation is left in the ideal case, and then the fast Fourier transform (FFT) can be used to analyze the frequency component of the carrier deviation.

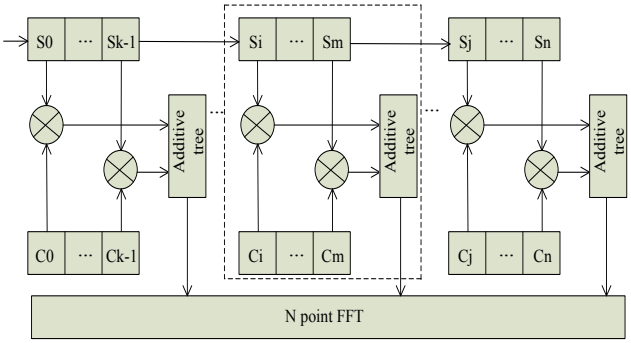

Figure 4: Principle diagram of PMF+FFT capture method

The PN-code phase, carrier frequency difference, and navigation message of the received signal can be obtained preliminarily after the process of spread spectrum capture. However, the PN-code ranging requires an accurate PN-code phase, because the ranging accuracy is in direct proportion to the estimation accuracy of the code phase. This paper discusses a fast accurate estimation algorithm for the PN-code phase and carrier frequency in case of the short-pulse communication below.

3.2 Fine estimation of the PN-code phase and carrier frequency

Fast, accurate estimation is required for the pseudo-random sequence code phase as the short-pulse communication is used for the system. The fine estimation of the PN-code phase and carrier frequency determines the ranging accuracy. For continuous spread spectrum signals, such as GNSS and DSSS signals with a long communication pulse duration, the carrier is usually tracked by PLL+FLL, and the PN-code by DLL loop, so as to achieve the fine estimation of carrier frequency and PN-code phase [Yang, Zhu et al. (2014); Liu, Zhang, Zhu et al. (2013); Ma, Wang, Li et al. (2012)]. Since the tracking loop requires a certain locking time, it is not suitable for the burst short-pulse communication mode.

In this paper, the latest maximum likelihood joint estimation (MLE) algorithm is used to calculate the carrier Doppler shift and accurate PN-code phase. Upon the completion of signal capture and the rough estimation of carrier and PN-code phases, the start and end moments of signals in a PN-code period can be determined preliminarily. The baseband

processing unit stores the sampled signal in a PN-code period to construct a function of maximum likelihood estimation (MLE) values, for which the optimal solutions of the PN-code phase and carrier frequency can be calculated with the optimization algorithm. The Levenberg-Marquart algorithm, one of the most efficient calculation methods for MLD, can be used for a solution [Won, Pany and Eissfeller (2012)].

4 Positioning principle of response-type ground-based area navigation

As mentioned above, the aircraft navigation terminal calculates the distance of the aircraft from the ground responder at the moment of a positioning request through response communication. The uplink signal includes the accurate coordinates of the ground responder. According to the principle of space geometry, the exact position of the point in the vector space can be accurately measured and determined if the space vector lengths of one point to multiple fixed points in the space are known.

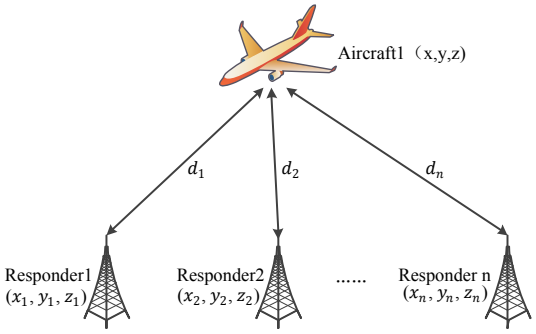

Figure 5: Composition block diagram of a response-type ground-based navigation system

As shown in Fig. 5, *S1-S3* denotes four ground responders with the coordinates of (x_i, y_i, z_i), and d_1-d_4 denote the distances from each ground responder to the aircraft navigation terminal. According to FIG. 5 above, the following Eq. (13) can be presented:

$$d_i = \sqrt{(x_i - x)^2 + (y_i - y)^2 + (z_i - z)^2} \tag{13}$$

Similarly, based on the ranging information from the aircraft to other ground responders, the following Eq. (14) can be presented:

$$\begin{aligned} d_1 &= \sqrt{(x_1 - x)^2 + (y_1 - y)^2 + (z_1 - z)^2} \\ d_2 &= \sqrt{(x_2 - x)^2 + (y_2 - y)^2 + (z_2 - z)^2} \\ &\vdots \\ d_n &= \sqrt{(x_n - x)^2 + (y_n - y)^2 + (z_n - z)^2} \end{aligned} \tag{14}$$

To calculate the equation set above by using a computer, linearization is required, and then iterative solution shall be performed [Elliott and Hegarty (2006); Wang, Kong, Guan et al. (2019)]. For the distance equation of any pseudolite, the position of the aircraft is assumed as (x_0, y_0, z_0) firstly, which can be linearized by Taylor expansion as below:

$$\begin{aligned}\Delta di &= di - \overset{\Lambda}{di} \\ &= \frac{x_i - x}{\overset{\Lambda}{di}}\Delta x + \frac{y_i - y}{\overset{\Lambda}{di}}\Delta y + \frac{z_i - z}{\overset{\Lambda}{di}}\Delta z + \varepsilon_i\end{aligned} \tag{15}$$

$$\begin{aligned}\Delta d_1 &= a_{x1}\Delta x + a_{y1}\Delta y + a_{z1}\Delta z + \varepsilon_1 \\ \Delta d_2 &= a_{x2}\Delta x + a_{y2}\Delta y + a_{z2}\Delta z + \varepsilon_2 \\ &\vdots \\ \Delta d_n &= a_{xn}\Delta x + a_{yn}\Delta y + a_{zn}\Delta z + \varepsilon_n\end{aligned} \tag{16}$$

$$\Delta d = \begin{pmatrix}\Delta d_1 \\ \Delta d_2 \\ \vdots \\ \Delta d_n\end{pmatrix}, \quad \Delta X = \begin{pmatrix}\Delta x \\ \Delta y \\ \Delta z\end{pmatrix}, \quad G = \begin{pmatrix}a_{x1} & a_{y1} & a_{z1} \\ a_{x2} & a_{y2} & a_{z2} \\ & \vdots & \\ a_{xn} & a_{yn} & a_{zn}\end{pmatrix}$$

The equation Eq. (16) can be solved with the least square method, as shown in Eq. (17) below.

$$\Delta \overset{\Lambda}{X} = \left(G^T G\right)^{-1} G^T \Delta d \tag{17}$$

The amount of position correction $\Delta \overset{\Lambda}{X}$ which can be obtained by each solution corrects the assumed initial position coordinates and the accurate position coordinates of the aircraft through convergence after several iterative operations.

5 The velocity measurement method of the concealed ground-based area navigation system

The actual flight velocity of the aircraft can be calculated after the carrier Doppler frequency of the aircraft to each ground responder and the position coordinates of the aircraft are determined. The uplink carrier Doppler frequency value of the aircraft received from the *ith* ground responder is as shown in Eq. (18) below:

$$f_{di} = DC_i * v + n_i \tag{18}$$

where $DC_i = \left[-\frac{x}{r_i}, -\frac{y}{r_i}, -\frac{z}{r_i}\right]$ is the radial direction cosine vector between the *ith* ground responder and aircraft; $v = \left[v_x, v_y, v_z\right]^T$ is the velocity vector of the aircraft; r_i is the distance between the ground responder and aircraft; n_i is the noise item; $\left[x_i, y_i, z_i\right]$ refers to the position coordinates of the *ith* ground responder; $\left[x, y, z\right]$ denotes the position coordinates of the aircraft.

It is assumed that the aircraft can acquire the carrier Doppler observations of a total of *m* ground responders, and the following can be obtained according to Eq. (18):

$$\begin{aligned} f_{d1} &= DC_1 * v + n_1 \\ f_{d2} &= DC_2 * v + n_2 \\ &\vdots \\ f_{dm} &= DC_m * v + n_m \end{aligned} \tag{19}$$

If it is defined that

$$f_d = \begin{bmatrix} f_{d1} \\ f_{d2} \\ \vdots \\ f_{dm} \end{bmatrix}, \quad H = \begin{bmatrix} DC_1 \\ DC_2 \\ \vdots \\ DC_m \end{bmatrix}, \quad n = \begin{bmatrix} n_1 \\ n_2 \\ \vdots \\ n_m \end{bmatrix}$$

The equation set Eq. (19) can be presented in the form of a matrix, i.e.

$$f_d = Hv + n \tag{20}$$

The velocity of the aircraft can be solved directly with the least square method, as shown in Eq. (21) below [Elliott and Hegarty (2006); Li, Chen, Gao et al. (2018)]:

$$\hat{v} = \left(H^T H\right)^{-1} H^T f_d \tag{21}$$

6 Concealed communication method with spread spectrum and frequency hopping technology

In order to increase the concealment characteristic of the system, the frequency hopping communication mode is adopted for both the uplink and downlink signals of the system, that is, the carrier frequency of each signal transmitted for each communication by the aircraft navigation terminal is different, and that of the uplink transmitting signal of the ground responders is different as well. Such a design will greatly improve the anti-interference and anti-reconnaissance performances of the system.

The aircraft navigation terminal is the central control unit for the entire frequency-hopping spread spectrum communication. The downlink and uplink frequency hopping patterns are bound in the aircraft navigation terminal. During the flight, the downlink signals transmitted in sequence according to the frequency hopping patterns contains the uplink carrier frequency information that shall be transmitted by the ground responder. The ground responders transmit the uplink signals according to the received frequency hopping information, and the entire system realizes the frequency synchronization of frequency hopping communication.

7 Conclusion

In this paper, the model of the concealed navigation system is established based on the response communication mode, and the working principle of this navigation system is analyzed. Using short-pulse communication, this system is silent at ordinary times, and the spread spectrum and frequency hopping technologies are adopted for the communication link, so the system has strong anti-reconnaissance and anti-jamming performances. In order

to realize the fast accurate estimation of the carrier frequency and PN-code phase of short-pulse DSSS signals, the PMF+FFT method is proposed to capture the signal and estimate the rough values of carrier frequency and PN-code phase, then the LM algorithm is used to solve the accurate estimation values of the carrier Doppler frequency and PN-code delay. Using this algorithm, the carrier frequency and PN-code phase can be estimated accurately in a PN-code period.

Due to the large transmission delay of the response communication mode, there is a big error when the common navigation algorithm is used for the positioning and velocity measurement of a high-velocity aircraft. A new algorithm is proposed in this paper. By calculating the radial velocity and compensating the ranging error caused by the motion, the algorithm can eliminate the influence of the response communication delay on the positioning of a high-velocity moving target and realize the precise positioning and velocity measurement of such high-velocity aircraft. In practical application, a reasonable layout shall be adopted to achieve an ideal navigation effect.

Funding Statement: The authors received no specific funding for this study.

Conflicts of Interest: The authors declare that they have no conflicts of interest to report regarding the present study.

References

An, X.; Lü, X.; Yang, L.; Zhou, X.; Lin, F. (2019): Node state monitoring scheme in fog radio access networks for intrusion detection. *IEEE Access*, vol. 7, pp. 21879 - 21888.

Elliott, D. K.; Hegarty, C. (2006): *Understanding GPS Principles and Applications.* Artech House.

Gong, C.; Lin, F.; Gong, X.; Lu, Y. (2020): Intelligent cooperative edge computing in the internet of things. *IEEE Internet of Things Journal*.

https://doi.org/10.1109/JIOT.2019.2957124.

Hui, H.; Zhou, C.; Xu, S.; Lin, F. (2020): A novel secure data transmission scheme in industrial internet of things. *China Communications*, vol. 17, no. 1, pp. 73-88.

Li, W. J.; Chen, Z. Y.; Gao, X. Y.; Liu, W.; Wang, J. (2018): Multimodel framework for indoor localization under mobile edge computing environment. *IEEE Internet of Things Journal*, vol. 6, no. 3, pp. 4844-4853.

Lin, F.; Zhou, Y.; An, X.; You, I.; Choo, K. C. (2018): Fair resource allocation in an intrusion-detection system for edge computing: ensuring the security of internet of things devices. *IEEE Consumer Electronics Magazine*, vol. 7, no. 6, pp. 45-50.

Lin, F.; Zhou, Y.; Pau, G.; Collotta, M. (2018): Optimization-oriented resource allocation management for vehicular fog computing. *IEEE Access*, vol. 6, pp. 69294-69303.

Lin, Y.; Zhu, Y. (2014): A FLL-PLL cooperative GNSS weak signal tracking framework. *Applied Mechanics and Materials*, vol. 551, pp. 470-477.

Liu, Y.; Zhang, J.; Zhu, Y. (2013): Weak satellite signal tracking loop based on traditional tracking framework. *Wireless Personal Communications*, vol. 70, pp. 1761-1775.

Ma, W. Z.; Wang, Z.; Li, Y. R.; Zhang, W. (2012): Research on code tracking loop algorithm of GPS. *Applied Mechanics and Materials*, vol. 229, no. 231, pp. 1556-1559.

Medhane, D. V.; Sangaiah, A. K.; Hossain, M. S.; Muhammad, G.; Wang, J. (2020): Blockchain-enabled distributed security framework for next generation IoT: an edge-cloud and software defined network integrated approach. *IEEE Internet of Things Journal.* https://doi.org/10.1109/JIOT.2020.2977196.

Qi, J.; Luo, F.; Song, Q. (2014): Fast acquisition method of navigation receiver based on folded PMF-FFT. *IEEE Computers, Communications and IT Applications Conference,* Beijing, China.

Tang, Q.; Wang, K. Z.; Song, Y.; Li, F.; Park, J. H. (2019): Waiting time minimized charging and discharging strategy based on mobile edge computing supported by software defined network. *IEEE Internet of Things Journal*.

Wang, B.; Kong, W.; Guan, H.; Xiong, N. N. (2019): Air quality forecasting based on gated recurrent long short term memory model in internet of things. *IEEE Access*, vol. 7, no. 1, pp. 69524-69534.

Wang, B.; Kong, W.; Li, W.; Xiong, N. N. (2019): A dual-chaining watermark scheme for data integrity protection in Internet of Things. *Computers, Materials & Continua*, vol. 58, no. 3, pp. 679-695.

Won, J. H.; Pany, T.; Eissfeller, B. (2012): Iterative maximum likelihood estimators for high-dynamic GNSS signal tracking. *IEEE Transactions on Aerospace and Electronic Systems*, vol. 48, no. 4, pp. 2875-2893.